Original Article

The Most Appropriate Time Delay after Microbubble Contrast Agent Intravenous Injection to Maximize Liver Metastasis Conspicuity on Contrast-Enhanced Ultrasound

Emilio Quaia[1]*, Antonio Giulio Gennari[2]

[1]Department of Radiology, Edinburgh Imaging Facility Queen's Medical Research Institute, University of Edinburgh, Edinburgh EH16 4TJ, Scotland, UK, [2]Department of Radiology, Cattinara Hospital, University of Trieste, 34149 Trieste, Italy

Abstract

Purpose: To identify the most appropriate time delay after microbubble contrast agent injection to maximize liver metastasis conspicuity on contrast-enhanced ultrasound (CEUS). **Methods:** Twenty-five consecutive patients (12 male and 13 female; age: 50 ± 13 years) with a known primary tumor and evidence of liver metastases on unenhanced ultrasound (US) underwent CEUS. CEUS consisted of continuous liver parenchyma scanning during arterial (15–35 s after microbubble injection), portal venous (40–120 s), and late phase (from 120 s up to microbubble disappearance). Subjective conspicuity index (ranging from 1 to 5) and objective conspicuity index (I_{lesion}–I_{liver}/I_{liver}, I = signal intensity) were calculated on reference frames selected on arterial phase and every 20 s on portal venous and late phase. **Results:** A total number of 40 liver metastases were identified after microbubble injection. The highest liver metastasis conspicuity was observed on early portal venous phase (40–60 s after microbubble injection) both on visual (mean subjective conspicuity index ± standard deviation [SD] = 4.36 ± 0.75, reader 1; 4.25 ± 0.65, reader 2) and quantitative analysis (mean objective conspicuity index ± SD = −0.99 ± 0.001). **Conclusion:** The early portal venous phase (40–60 s after microbubble injection) provides the best liver metastases' conspicuity after microbubble contrast agent injection.

Keywords: Liver, metastasis, microbubble contrast agent

Introduction

The accurate assessment of liver metastatic disease is important for the treatment planning of primary malignancies. Unenhanced gray-scale ultrasound (US) is routinely used as the first-line imaging modality in liver metastasis detection in patients with a known primary cancer, even though it presents a limited sensitivity (from 40% to 60%).[1-3]

Contrast-enhanced US (CEUS)[4] was previously shown to improve the overall accuracy of US in liver metastases' diagnosis.[1-3,5-7] The CEUS sensitivity in detecting liver metastases is 79%–100% which is comparable with CT.[8-11] Portal venous phase begins 30–45 s after microbubble injection and lasts up to 120 s after injection, while late phase begins >120 s after microbubble injection and lasts up to microbubble disappearance from the bloodstream (approximately 4–6 min after injection).[12]

Liver metastases can be detected and characterized reliably as hypoenhancing lesions during the portal venous and late phases after microbubble contrast agent injection.[12]

The proper technical settings, mechanical index, signal persistence, focal zone position, etc., to obtain the highest possible enhancement of liver parenchyma after microbubble injection are well established.[13] However, it was not shown yet what is the best time delay after microbubble contrast agent injection to obtain the highest liver metastasis visibility over liver parenchyma background. The definition of the best temporal window to visualize liver metastases could allow to select the best time delay to detect liver metastases

Received: 10-07-2017 **Accepted:** 09-11-2017 **Available Online:** 14-09-2018

Access this article online

Quick Response Code:

Website: www.jmuonline.org

DOI: 10.4103/JMU.JMU_12_17

Address for correspondence: Dr. Emilio Quaia, Edinburgh Imaging Facility Queen's Medical Research Institute, University of Edinburgh, 47 Little France Crescent, Edinburgh EH16 4TJ, Scotland, UK. E-mail: equaia@exseed.ed.ac.uk

This is an open access journal, and articles are distributed under the terms of the Creative Commons Attribution-NonCommercial-ShareAlike 4.0 License, which allows others to remix, tweak, and build upon the work non-commercially, as long as appropriate credit is given and the new creations are licensed under the identical terms.

For reprints contact: reprints@medknow.com

How to cite this article: Quaia E, Gennari AG. The most appropriate time delay after microbubble contrast agent intravenous injection to maximize liver metastasis conspicuity on contrast-enhanced ultrasound. J Med Ultrasound 2018;26:128-33.

after microbubble contrast agent injection and could allow to minimize microbubble rupture by avoiding useless prolonged US scanning.

The aim of the present study was to identify the most appropriate time delay after microbubble injection to maximize liver metastasis conspicuity on CEUS.

Methods

This retrospective observational study was approved by the ethics committee of the institute in which the study was performed and written informed consent was obtained from all patients.

Through a review of clinical records of patients imaged between January 1, 2014, and January 1, 2016, we identified all patients with evidence of liver metastases on unenhanced US and scanned subsequently by CEUS. To be eligible for this study, patients had to meet these inclusion criteria: (1) evidence of single or multiple (<5 in number) discrete noncoalescent liver metastases appearing unequivocally hypoenhancing on portal venous phase from 40 s after microbubble injection; (2) no more than 14 days between unenhanced US and CEUS; and (3) lesions subsequently proven as liver metastases based on contrast-enhanced CT or MR or histology obtained no more than 2 weeks after CEUS.

Of the 55 patients who were deemed initially eligible for the study, 30 patients were excluded according to the following criteria: an interval of more than 14 days between unenhanced US and CEUS (n = 3); an interval of more than 14 days between CEUS and contrast-enhanced CT or MR or even biopsy (n = 5); patients with widespread metastatic liver involvement or patients with multiple coalescent multiple liver metastases which could limit the assessment of conspicuity of single lesions (n = 5); patients previously treated for liver metastases by thermal ablation or surgical procedures (n = 2); liver steatosis due to the increased probability of high liver metastasis conspicuity even on unenhanced US and limited liver parenchyma enhancement after microbubble injection (n = 3); patients receiving chemotherapy (n = 9); incomplete visibility of the liver parenchyma at unenhanced US due to intervening bowel gas and patient body habitus (n = 2); and liver cirrhosis or chronic liver disease diagnosed by tru-cut needle biopsy (n = 1).

Therefore, 25 consecutive patients (12 male and 13 female; age: 50 ± 13 years) were finally included, with the following primary tumors: colorectal adenocarcinoma (n = 16 patients), lung adenocarcinoma or squamous cell carcinoma (n = 6), breast ductal or lobular carcinoma (n = 2), and pancreas adenocarcinoma (n = 1).

Unenhanced and contrast-enhanced ultrasound examination

US examination was conducted by iU22 xMATRIX Ultrasound System (Philips Healthcare, Bothell, WA) by using a broadband 256 elements convex-array transducer (C5-2, 50 mm × 10 mm). Unenhanced gray-scale US was performed by employing noise and speckle reducing tissue harmonic and compound modes through transverse, longitudinal, and intercostal scans.

CEUS was conducted after manual intravenous (IV) bolus injection of sulfur hexafluoride-filled microbubbles (2.4 mL) in a peripheral forearm vein followed by a 10–20 ml normal saline flush. Scanning time from microbubble contrast IV injection was registered. The scanning technique consisted in continuous low transmit power insonation (mechanical index = 0.08) from 15 to 35 s (arterial phase), from 40 to 120 s (portal venous phase), and from 120 s up to microbubble disappearance after microbubble injection (late phase).

All technical parameters were set at the same value: power-modulated pulse inversion technology; central transmit frequency 3.2–3.7 MHz; dynamic range 60–65 dB; echo-signal gain below noise visibility; 10–13 frames per second, signal persistence turned on; and one focus set at a depth of 8–10 cm from the abdominal surface at the level of the diaphragm.

One uncompressed digital imaging and communications in medicine (DICOM) multiframe digital cine-clip (15 frames/s) was acquired during arterial phase, while separate DICOM cine-clips (20 s in duration each) were acquired during portal venous and late phase. Each DICOM cine-clip was transferred to the picture archiving and communication system (PACS) of the radiology department.

Ultrasound image assessment

DICOM cine-clips were reviewed on screen (Intel, Pentium 4 with 20-inch TFT display, Santa Clara, Calif, USA). All readings were performed on a PACS-integrated workstation (19-inch TFT display, resolution 2560 × 1600 pixels) at a central location by using a proprietary software package (Ebit Sanita AET, Genoa, Italy).

Two registered diagnostic radiologists affiliated to the center in which the study was performed and who were involved in patient scanning – one reference radiologist (EQ) with 20 years of experience on abdominal CEUS and a chief resident with 4 years of experience on CEUS – performed visual analysis. All readers were not blinded to the clinical history of the patients and to the results of the other imaging examinations. The visual assessment was done independently from the two readers.

First, metastatic lesions were localized in a liver segment according to the Bismuth and Couinaud classification[14,15] on schematic liver charts. The diameter of each lesion was measured by calipers, and contrast enhancement patterns observed on arterial phase – hyperenhancing, hypoenhancing, nonenhancing, rim enhancement – were classified according to the European Federation of Societies for Ultrasound in Medicine and Biology (EFSUMB) guidelines.[12] The overall metastatic lesion conspicuity over the liver parenchyma background was visually assessed according to a subjective conspicuity index ranging from 1 (poor visibility, lesion(s) presenting the same echogenicity of the adjacent liver parenchyma), 2–4 (progressively higher lesion visibility over

the liver parenchyma background), up to 5 (maximal lesion visibility with liver metastases appearing as unenhancing lesions within the enhancing liver parenchyma) during the different time frames (arterial phase and every 20 s on portal venous and late phase).

Second, 3 months after completion of visual analysis, the reference radiologist (EQ) performed a quantitative analysis of echo power by using a proprietary software package (VueBox, Version 4.3, Bracco, Geneva, Switzerland).[16] Each digital cine-clip was transferred to an encrypted USB device and then to a computer (Intel, Pentium 4, Santa Clara, CA) connected to PACS and was used for the quantitative analysis. VueBox linearizes compressed DICOM images through application of an antilog function within the linear range of the microbubble concentration versus video-intensity relation. The US video intensity was measured in linear arbitrary units.

For each patient, one marker lesion was identified by the reader according to diameter and best lesion visualization after microbubble injection. DICOM cine-clips recorded during the different dynamic phases were reviewed by the reader involved in quantitative analysis with the possibility to scroll images to identify those image frames in which the marker lesion revealed the better conspicuity. The image frame in which the marker lesion revealed the best lesion conspicuity was selected for the quantitative analysis. In each image, a manually defined circular (2300–4110 pixels, mean 3430 pixels) region of interest (ROI) was drawn encompassing the marker lesion avoiding artifacts [Figure 1]. In those metastatic lesions presenting a peripheral rim enhancement during the hepatic arterial phase, the lesion ROI did not include the peripheral-enhancing tissues.

A second ROI, serving as internal reference, was drawn beside at the same depth or immediately above the marker lesion encompassing the adjacent liver parenchyma avoiding liver vessels and artifacts [Figure 1]. Then, an objective conspicuity index was calculated from the difference in absolute linear scale values between the lesion and the adjacent liver parenchyma over the signal intensity measured on the liver parenchyma ($I_{lesion} - I_{liver}/I_{liver}$, I=signal intensity, where I means signal intensity in linear arbitrary units) during the different phases (arterial phase and every 20 s on portal venous and late phase). Two sessions, each of 3 h and separate by two days, were necessary to complete the analysis.

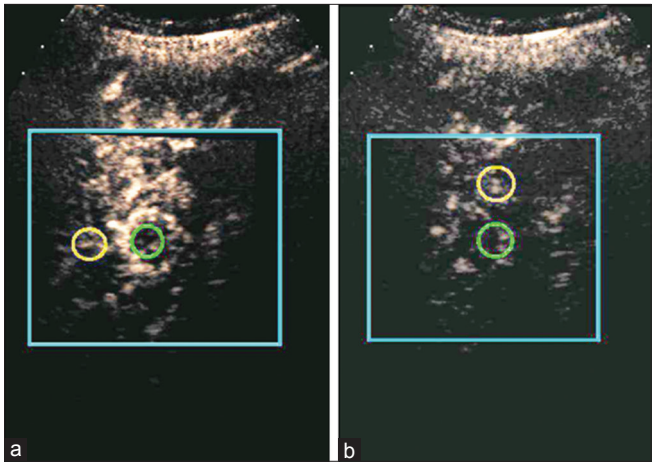

Figure 1: Objective analysis. The external square delimits the whole region of liver parenchyma selected for analysis. One circular region of interest is placed over the marker lesion while another region of interest is drawn over the liver parenchyma beside the marker lesion (a) or over the liver parenchyma immediately above the marker lesion (b)

Contrast-enhanced computed tomography and magnetic resonance imaging

Liver-computed tomography (CT) examination (Brilliance iCT 256, Philips, Best, The Netherlands) was performed in 16 patients with the following technical parameters: rotation time, 270 ms; beam collimation, 128 mm × 2 mm × 0.625 mm; normalized pitch, 0.975; z-axis coverage, 160 mm; reconstruction interval, 0.3 mm; section reconstruction thickness, 3 mm; tube voltage, 120 kV; tube current, 280–400 mA depending on patient size; and field of view, 40 cm. CT scan was performed after nonionic-iodinated contrast agent injection (4 ml/s; 120–150 ml; 350 mg of iodine per ml; Iomeron 350; Bracco, Milan, Italy) during arterial (25–30 s delay), portal venous (70–90 s delay), and late phase (120 s to 5 min delay).

Liver magnetic resonance (MR) imaging was performed in 9 patients on a 1.5-T MR imager (Achieva; Philips Healthcare, Best, The Netherlands). MR images were acquired on transverse plane with a combined four channel anteroposterior phased-array surface coil. We obtained respiratory-triggered T2-weighted single-shot turbo spin-echo (TR/TE, infinite/80), T2-weighted (TR/TE, 350/71) and T1-weighted in-phase and out-of-phase (TR/TE, 332/4.6–2.3 ms) fast-field echo, and dynamic fat-suppressed T1-weighted high-resolution isotropic volume examination sequences with a 3D acquisition, before and after gadobenate dimeglumine injection (0.1 mmol/kg; 2 mL/s) on arterial phase (starting with a 5-s delay from the contrast visualization in the abdominal aorta) and on portal venous, late, and hepatobiliary phase which were initiated at 70 s, 180 s, and 1–2 h (mean, 1.2 h), respectively, after the start of injection of contrast agent.

CT or MR images were reviewed by the reference radiologist who matched the liver metastases detected on CEUS with liver metastases detected on CT or MR images based on lesion location and dimension in each patient. The evidence of hyperenhancement or rim enhancement on hepatic arterial phase and the evidence of lesion hypoenhancement on the portal venous and late phase (with the absence of contrast uptake on the hepatobiliary phase) were considered diagnostic for liver metastases.[17]

In 3 patients with one liver metastasis each in whom CT scan was not conclusive (equivocal isodense or hypodense lesion appearance during the portal venous and delayed phase), percutaneous US-guided biopsy was performed by using 18-gauge modified Menghini needle. Two histologic samples

were obtained from each lesion, fixed in formalin, embedded in paraffin, and stained with H and E and the Masson trichrome method. A pathologist with 15 years of experience in pathologic examination of hepatobiliary diseases retrospectively reviewed the pathology slides and the macroscopic pictures of the resected specimens with no knowledge of the imaging findings.

Statistical analysis

Statistical analysis was performed by a computer software package (Med Calculator, version 12.2.1, Mariakerke, Belgium).

The weighted kappa statistic[18,19] was calculated to assess inter-reader agreement in the overall lesion visibility from both readers. Agreement was graded as poor ($\kappa < 0.20$), fair (≥ 0.20 and <0.40), moderate (≥ 0.40 and <0.60), good (≥ 0.60 and <0.80), or very good (≥ 0.8–1).

Results

A total number of 40 metastases (mean diameter, 2.5 cm ± 0.96; range, 1–4.2 cm) with a mean of 1.6 lesions per patient (range 1–2 lesions) were identified after microbubble injection. Twenty-five marker lesions were identified. All liver metastases detected by CEUS were confirmed by CT or MR imaging.

On arterial phase after microbubble injection, 20 metastatic lesions revealed homogeneous or heterogeneous hyperenhancement, 18 lesions revealed peripheral rim enhancement, and 2 lesions appears persistently hypoenhancing.

Both on portal venous and late phase after microbubble injection, all liver metastases appeared hypoenhancing. No difference in terms of portal venous or delayed phase vascularity was observed since all liver metastases appeared unequivocally hypoenhancing on portal venous and delayed phase, independently from their diameter and enhancement pattern on arterial phase.

Table 1 shows the results of visual analysis. The best overall metastatic lesion conspicuity (mean subjective conspicuity index ± standard deviation [SD] = 4.36 ± 0.75, reader 1; 4.25 ± 0.65, reader 2) was observed during portal venous phase in the timeframe from 40 to 60 s after microbubble injection [Figure 2]. The agreement between readers was optimal ($k = 0.85$).

Table 2 shows the results of quantitative analysis. The highest objective conspicuity of liver metastases (mean objective conspicuity index ± SD = −0.99 ± 0.001) was measured during the early portal venous phase in the timeframe from 40 to 60 s after microbubble injection.

Discussion

Detection of liver metastases is an important issue in defining the most appropriate treatment in oncologic patients, and CEUS was preliminary shown to improve the overall accuracy of baseline US in liver metastases' diagnosis.[1-3,5-11] The improved detection of liver metastases by CEUS was confirmed also

Table 1: Mean subjective conspicuity index±standard deviation of liver metastases

Timeframes	First reader	Second reader
Arterial phase (15-35 s)	3.37±2.87	3.15±1.15
Portal venous phase (40-60 s)	4.36±0.75	4.25±0.65
Portal venous phase (>60-80 s)	4.16±0.55	4.18±0.25
Portal venous phase (>80-100 s)	3.36±0.25	3.25±0.65
Portal venous phase (>100-120 s)	3.16±0.25	3.1±0.35
Late phase (>120 s)	2.38±0.75	2.45±0.65

Mean subjective conspicuity index±SD. SD: Standard deviation

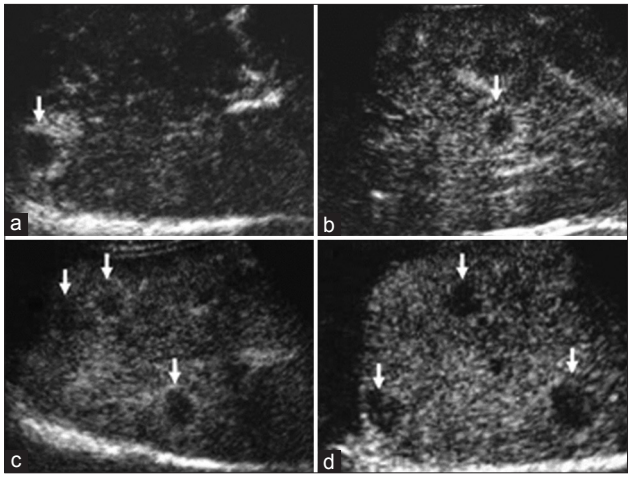

Figure 2: Progressive increase in visual conspicuity of liver metastases. (a) Arterial phase –- 15 s after sulfur hexafluoride-filled microbubble injection. (b-d) Portal venous phase - Progressive increase in lesion conspicuity from 40 s (b), through 45 s (c), up to 55 s after microbubble injection (d)

in patients who received chemotherapy[20] and in patients with fatty infiltration of the liver.[21] The increased detection of liver metastases on CEUS compared to unenhanced US is determined by persistent contrast enhancement in the adjacent normal liver parenchyma due to harmonic frequencies produced by microbubble insonation. During the portal venous phase, microbubbles are pooling within the hepatic sinusoids and liver parenchyma enhances, while liver metastases, devoid of hepatic sinusoids, appear as hypoenhancing lesions. The conspicuity of liver metastases over the liver parenchyma background determines the visibility of liver metastases and, consequently, their detectability.

In this study, we showed that temporal window in which liver metastases reveal the highest visibility corresponds to the early portal venous phase, namely from 40 to 60 s after microbubble injection. In particular, we found that liver metastasis conspicuity is not constant over the different dynamic phases, even within the same portal venous phase. On arterial phase, the evidence of hyperenhancement in a high number of liver metastases determined the positive value of the objective conspicuity index which became negative on the portal venous and late phase due to the hypoenhancing appearance of liver metastases. The highest liver metastasis

Table 2: Results of objective analysis

Timeframes (s)	Mean±SD		
	Lesion signal intensity	Liver signal intensity	Objective conspicuity index
Arterial phase (15-35)	5176±6254.5	1552±554.8	2.69±4.85
Portal venous phase (40-60)	174.2±64.62	517,600±625,451.7	−0.99±0.001
Portal venous phase (>60-80)	166±63.41	15,796±20,936.48	−0.96±0.02
Portal venous phase (>80-100)	133.6±40.58	4334±6410.98	−0.93±0.04
Portal venous phase (>100-120)	112.6±29.65	1648±2226.33	−0.89±0.06
Late phase (>120)	95.04±25.19	838±921.42	−0.80±0.16

Mean objective conspicuity index expressing the difference in echogenicity of metastatic lesions in comparison with adjacent liver parenchyma during the different time frames. SD: Standard deviation

conspicuity was observed on the early portal venous phase since, apparently, a time of 40–60 s after injection is needed for the complete contrast washout from liver metastases and for the achievement of the highest enhancement on the adjacent liver parenchyma.

To minimize microbubble rupture, US scan should be stopped and resumed several times (e.g., every 20 s) after microbubble injection, particularly on the portal venous phase[12] and even when a very low mechanical index is used. According to our results, the best temporal window to maximize liver metastasis detection corresponds to the early portal venous phase, and there is no need to prolong liver insonation during the following seconds of the portal venous phase and during the following late phase. On the other hand, the operator should play the highest attention to detect liver metastases during the early portal venous phase since liver metastasis visibility becomes progressively lower after 60 s from microbubble injection due to the progressively decreasing liver parenchyma enhancement, especially if continuous insonation is employed.

In this study, we used sulfur hexafluoride-filled microbubbles since SonoVue is presently the only microbubble contrast agent licensed in Europe. Consequently, our results can be applied only to those CEUS examination obtained after sulfur hexafluoride-filled microbubble injection. On the other hand, the results of the present study could not be reproducible if other microbubble contrast agents are injected, especially if these agents have hepatospecific properties (e.g., Sonazoid).[22]

Change of microbubble contrast agent dose, level of acoustic power insonation (namely, mechanical index value), US equipment, and contrast-specific mode may all modify liver metastasis conspicuity on CEUS, although we used the registered dose of sulfur hexafluoride-filled microbubbles for liver imaging which is also supported by EFSUMB.[23] Moreover, we employed state-of-the-art US equipment and contrast-specific mode which both reflect the clinical practice in a tertiary referral hospital.

In this study, the main limitations correspond to its retrospective nature, the limited number of patients with metastatic liver lesions due to multiple exclusion criteria employed, and to inclusion of only patients with liver metastases which were evident at gray-scale and contrast-enhanced US and subsequently proven at CT or MR which could overestimate the capabilities of CEUS in liver metastases' detection. However, the aim of the present study was to assess the best temporal window providing the best liver metastasis conspicuity after microbubble injection instead of diagnostic accuracy of contrast-enhanced US.

Conclusion

The early portal venous phase (40–60 s after microbubble injection) provides the best liver metastases' conspicuity after microbubble contrast agent injection.

Financial support and sponsorship

Nil.

Conflicts of interest

There are no conflicts of interest.

References

1. Quaia E, D'Onofrio M, Palumbo A, Rossi S, Bruni S, Cova M, *et al.* Comparison of contrast-enhanced ultrasonography versus baseline ultrasound and contrast-enhanced computed tomography in metastatic disease of the liver: Diagnostic performance and confidence. Eur Radiol 2006;16:1599-609.
2. Dietrich CF, Kratzer W, Strobe D, Danse E, Fessl R, Bunk A, *et al.* Assessment of metastatic liver disease in patients with primary extrahepatic tumors by contrast-enhanced sonography versus CT and MRI. World J Gastroenterol 2006;12:1699-705.
3. Oldenburg A, Hohmann J, Foert E, Skrok J, Hoffmann CW, Frericks B, *et al.* Detection of hepatic metastases with low MI real time contrast enhanced sonography and SonoVue. Ultraschall Med 2005;26:277-84.
4. Quaia E. Microbubble ultrasound contrast agents: An update. Eur Radiol 2007;17:1995-2008.
5. Harvey CJ, Blomley MJ, Eckersley RJ, Cosgrove DO, Patel N, Heckemann RA, *et al.* Hepatic malignancies: Improved detection with pulse-inversion US in late phase of enhancement with SH U 508A-early experience. Radiology 2000;216:903-8.
6. Mishima M, Toh U, Iwakuma N, Takenaka M, Furukawa M, Akagi Y, *et al.* Evaluation of contrast sonazoid-enhanced ultrasonography for the detection of hepatic metastases in breast cancer. Breast Cancer 2016;23:231-41.
7. Ruzzenente A, Conci S, Iacono C, Valdegamberi A, Campagnaro T, Bertuzzo F, *et al.* Usefulness of contrast-enhanced intraoperative ultrasonography (CE-IOUS) in patients with colorectal liver metastases after preoperative chemotherapy. J Gastrointest Surg 2013;17:281-7.
8. Cabassa P, Bipat S, Longaretti L, Morone M, Maroldi R. Liver metastases: Sulphur hexafluoride-enhanced ultrasonography for lesion detection: A systematic review. Ultrasound Med Biol 2010;36:1561-7.
9. Rafaelsen SR, Jakobsen A. Contrast-enhanced ultrasound vs.

multidetector-computed tomography for detecting liver metastases in colorectal cancer: A prospective, blinded, patient-by-patient analysis. Colorectal Dis 2011;13:420-5.
10. Larsen LP, Rosenkilde M, Christensen H, Bang N, Bolvig L, Christiansen T, *et al.* The value of contrast enhanced ultrasonography in detection of liver metastases from colorectal cancer: A prospective double-blinded study. Eur J Radiol 2007;62:302-7.
11. Cantisani V, Ricci P, Erturk M, Pagliara E, Drudi F, Calliada F, *et al.* Detection of hepatic metastases from colorectal cancer: Prospective evaluation of gray scale US versus SonoVue® low mechanical index real time-enhanced US as compared with multidetector-CT or Gd-BOPTA-MRI. Ultraschall Med 2010;31:500-5.
12. Claudon M, Dietrich CF, Choi BI, Cosgrove DO, Kudo M, Nolsøe CP, *et al.* Guidelines and good clinical practice recommendations for contrast enhanced ultrasound (CEUS) in the liver – Update 2012: A WFUMB-EFSUMB initiative in cooperation with representatives of AFSUMB, AIUM, ASUM, FLAUS and ICUS. Ultraschall Med 2013;34:11-29.
13. Liu JB, Wansaicheong G, Merton DA, Forsberg F, Goldberg BB. Contrast-enhanced Ultrasound Imaging: State of the Art. J Med Ultrasound 2005;13:109-26.
14. Bismuth H. Surgical anatomy and anatomical surgery of the liver. World J Surg 1982;6:3-9.
15. Couinaud C. The liver: Anatomical and surgical studies. Paris: Masson; 1957.
16. Tranquart F, Mercier L, Frinking P, Gaud E, Arditi M. Perfusion quantification in contrast-enhanced ultrasound (CEUS) – Ready for research projects and routine clinical use. Ultraschall Med 2012;33 Suppl 1:S31-8.
17. Federle MP. Diagnostic Imaging: Abdomen. Manitoba (Canada): Amirsys; 2004.
18. Cohen J. A coefficient of agreement for nominal scales. Educ Psychol Meas 1960;20:37-46.
19. Landis JR, Koch GG. The measurement of observer agreement for categorical data. Biometrics 1977;33:159-74.
20. Konopke R, Bunk A, Kersting S. Contrast-enhanced ultrasonography in patients with colorectal liver metastases after chemotherapy. Ultraschall Med 2008;29 Suppl 4:S203-9.
21. Bartolotta TV, Taibbi A, Picone D, Anastasi A, Midiri M, Lagalla R, *et al.* Detection of liver metastases in cancer patients with geographic fatty infiltration of the liver: The added value of contrast-enhanced sonography. Ultrasonography 2017;36:160-9.
22. Sugimoto K, Moriyasu F, Saito K, Taira J, Saguchi T, Yoshimura N, *et al.* Comparison of Kupffer-phase sonazoid-enhanced sonography and hepatobiliary-phase gadoxetic acid-enhanced magnetic resonance imaging of hepatocellular carcinoma and correlation with histologic grading. J Ultrasound Med 2012;31:529-38.
23. Piscaglia F, Nolsøe C, Dietrich CF, Cosgrove DO, Gilja OH, Bachmann Nielsen M, *et al.* The EFSUMB guidelines and recommendations on the clinical practice of contrast enhanced ultrasound (CEUS): Update 2011 on non-hepatic applications. Ultraschall Med 2012;33:33-59.